Modeling Broadband Electromagnetic Induction Responses of 2-D Multilayered Structures

Patricia Martinelli, Ana Osella, and Eugenia Lascano

***Abstract*—Dual-coil frequency-domain electromagnetic induction (EMI) systems are commonly used as detectors of buried metallic objects, but they are also increasingly used for environmental purposes such as detection of contaminant plumes and archaeological prospection. Usually, data are analyzed directly by visualizing the in-phase and quadrature components, and also by applying one-dimensional inversion methods. Besides, there exist three-dimensional (3-D) forward and inverse modeling codes based on finite-difference techniques, but these methods are not routinely applied because their computation cost for real geophysical situations is still too high. The computation cost is significantly lower for two-dimensional (2-D) structures since this problem is not 3-D but 2.5-D. Few 2.5-D methods have been published in the last years, based on finite-element techniques, but for the case of electric dipole sources. In this paper, the authors present a 2.5-D forward-modeling algorithm, based on Rayleigh–Fourier expansions, for calculating the response of 2-D multilayered earth with irregular boundaries to the magnetic-dipole sources. Using this code, the authors numerically simulated the dual-coil frequency-domain EMI response of a soil model that could be found in environmental research. They considered a buried nonmetallic object, conductive with respect to the host media, and calculated its response for different orientations of the transmitter and receiver coils. The best resolution for detecting and characterizing this object corresponded to the configuration in which the axes of the transmitter and receiver dipoles were parallel to the ground surface and perpendicular to the symmetry axis of the buried objects, and the axis of the instrument was parallel to that symmetry axis. Finally, the authors interpreted the field data from a profile exhibiting resistive anomalies, corresponding to underground contamination, by using their forward code and a trial-and-error procedure. This profile had been previously characterized through the inversion of dipole–dipole electrical data. They considered that result to select their starting multilayered model. They obtained a good correlation between the EMI data and the synthetic response of the final multilayered model. Besides, this model is consistent with the image of the electrical inversion. During the modeling process, the method showed to be practical and versatile and to have a good convergence.**

***Index Terms*—Discrete Fourier transforms, dual coil, electromagnetic induction (EMI), forward modeling, frequency domain, Rayleigh scattering, two-dimensional structures.**

Manuscript received November 8, 2005; revised August 5, 2005. This work was supported in part by Agencia Nacional de Promoción Científica y Tecnológica (ANPCyT).

P. Martinelli and A. Osella are with the Physics Department, Faculty of Sciences, University of Buenos Aires, Buenos Aires 1428, Argentina and also with the Consejo Nacional de Investigaciones Científicas y Técnicas (CONICET), Buenos Aires, Argentina.

E. Lascano is with the Physics Department, Faculty of Sciences, University of Buenos Aires, Buenos Aires 1428, Argentina.

Digital Object Identifier 10.1109/TGRS.2006.873746

I. Introduction

DUAL-COIL frequency-domain electromagnetic induction (EMI) systems are commonly used to detect buried metallic bodies, such as unexploded ordnance (UXO), because they are very sensitive to the presence of highly conductive structures. But they are also useful for environmental applications like contaminant detection, waste-site exploration, or archaeological prospection, since they are an alternative method to delimit anomalous zones. One of the main advantages of these systems is that they do not require direct contact with the ground and, therefore, are much faster than other EM methods. This is especially important when dealing with these kinds of targets because the surveyed area is usually too large compared to the lateral resolution required for shallow prospections. Though anomalous zones can be detected directly by a visualization of EMI data, much more information can be obtained if a quantitative analysis is added to the first qualitative result.

In recent years, several methods to calculate the EMI response of metallic bodies have been presented and applied to analyze and characterize the response of UXO [1]–[4]. In all these works, it is supposed that the objects are in free space. This is because metals usually are orders of magnitude more conductive than the common background media. In spite of that, obtaining accurate numerical results is difficult and requires extensive computation costs, since the very high conductivity of the bodies can destabilize the numerical solutions.

In environmental applications, conductivity contrasts are lower, and therefore, the background must be considered together with the targets. But this is also a complicated task mainly because the magnetic-dipole sources are very localized and generate three-dimensional (3-D) fields. Due to this reason, even at present, the usual approach to quantitatively interpret EMI data is to apply one-dimensional (1-D) inversion methods [5]. The use of these methods always brings more information than the mere observation of data and gives very good results in particular cases in which the soil structure can be regarded as being approximately 1-D. However, the soil structure is not 1-D in most cases. In those situations, better descriptions of the actual features of the subsurface may be obtained by applying forward or inverse methods that allow considering two-dimensional (2-D) or 3-D earth models. The calculation of the response to a 3-D magnetic-dipole source is a 2.5-D problem for a 2-D earth, while a fully 3-D problem for a 3-D earth. The first published solutions considered 2-D or 3-D bodies, having simple geometry, embedded in uniform or layered 1-D media (2.5-D methods: [6]–[8], 3-D methods: [9]–[11]). More than a decade after these pioneering works, a forward method based on finite-difference (FD) techniques was presented, which considers much more general 3-D

models [12]. Later, inversion algorithms were implemented for 3-D FD forward methods [13], [14]. But all of these 3-D FD codes are not routinely employed for the interpretation of EMI data because their computation cost is still too high for present-day common computers. On the other hand, the computation cost of 2.5-D modeling is significantly lower and actually becoming affordable moreover, taking into account that the earth's structure can be considered 2-D in many geophysical situations. Nevertheless, this subject received little attention in the literature in the last years. Only a few 2.5-D methods were presented, all for the case of electric dipole sources. Unsworth *et al.* [15] and Mitsuhata [16] published forward methods based on finite elements (FE), and later, Mitsuhata *et al.* [17] implemented an inversion code for their forward-modeling algorithm.

In general, FD forward codes consider models in which soil properties vary gradually between adjacent elements of a mesh. This is also the standard approach in inversion codes, based not only on FD but also on FE forward methods, which also seek for the smoothest model that fits the data. Imposition of smoothness constraints stabilizes the algorithms but could lead to unrealistic interpretations in situations in which it is known (from well-log data or archaeological excavations, for instance) that the underground structure consists of layers of nearly uniform conductivity separated by boundaries defining sharp resistivity contrasts [18]. In these cases, the use of Rayleigh–Fourier (RF) techniques is very appropriated. Though FEs also allow for discontinuities in soil properties, RF expansions are especially formulated for the modeling of multilayered structures with irregular boundaries.

Recently, we presented an RF method to calculate the EM response of 2-D structures as the ones described above to arbitrary 2-D and 3-D inducing fields [19]. Previously, we had also implemented RF magnetotelluric modeling algorithms for 2-D and 3-D structures [20], [21]. Here, by modifying the results presented in the work of Martinelli and Osella [19], we develop a 2.5-D RF method for calculating the dual-coil frequency-domain EM response of 2-D structures.

Afterward, we propose a soil model representing a structural feature that could be found in environmental applications, and by using this method, we numerically simulate its in-phase (HI) and quadrature (HQ) responses. We consider a nonmetallic embedded body, conductive with respect to the host medium, which could represent for instance a contaminant spill, and analyze the resolution of its responses for different orientations of the dipole source and receiver.

Finally, we apply this method to interpret field data acquired along a profile that crosses a zone where the soil presents resistive anomalies produced by contaminant material. To select the starting model of the subsurface structure, we used information from a geoelectrical dipole–dipole profile obtained along the same line. Then, we varied this model, using a trial-and-error procedure, until a good correlation between the data and synthetic response was achieved.

II. EMI Responses of 2-D Multilayered Structures

In this section, we obtain the dual-coil EMI responses of 2-D multilayered structures. The EMI system consists of two small coils, a transmitter, and a receiver separated by a constant distance, which is moved along a profile. The secondary field detected at the receiver is separated into HI and HQ components, which are expressed in parts per million (PPM) against the primary field. The depth of penetration is a function of the frequency ω, the distance between the emitter and the receiver, and the conductivity of the media. In the proposed model, each medium n, for $0 \leq n \leq N$, has a conductivity σ_n, dielectric permittivity ε_n, and magnetic permeability μ_n. The air (medium 0) has ε_0 and μ_0 equal to that of the free space, and $\sigma_0 = 0$. The air–earth interface corresponds to $z = 0$, where z is positive downward and y is the symmetry direction. The studied area has lengths L_x and L_y in the x and y directions, respectively. Layer boundaries are given there by smooth functions $z = S_n(x)$, with $1 \leq n \leq N-1$. The emitter has a magnetic-dipole moment $\overline{\mathfrak{M}}_e$ and a time dependence $\exp(i\omega t)$. It is located over the studied area at the position $\overline{r}_e = (x_e, y_e, z_e)$, with $z_e < 0$. Hence, inside each medium n, the electric $\overline{E}_n$ and magnetic $\overline{H}_n$ fields satisfy

$$\overline{\nabla} \times \overline{E}_n = -i\omega\mu_n \overline{H}_n \tag{1}$$

$$\overline{\nabla} \times \overline{H}_n = (\sigma_n + i\omega\varepsilon_n)\overline{E}_n. \tag{2}$$

In the air, these equations are valid except at the location of the source.

To solve the problem, we must extend the model outside the studied zone. We choose an extension that greatly simplifies the treatment. In this extended model, the interfaces S_n are even and periodic functions of x, and the external field $\overline{H}_{\text{ext}}$ is a periodic function of x and y. The periodicities in x and y are λ_x and λ_y, respectively. The studied zone is centered at $x = \lambda_x/4$ and $y = \lambda_y/4$. $\lambda_x/2$ and $\lambda_y/2$ must be greater than L_x and L_y, respectively, and such that the field produced by the emitter dipole at the boundaries of the area $0 \leq x \leq \lambda_x/2$, $0 \leq y \leq \lambda_y/2$ is negligible. We extend the interfaces as follows:

$$S_n(x) = \begin{cases} S_n(\lambda_x/4 - L_x/2), & \text{if } 0 \leq |x| \leq \lambda_x/4 - L_x/2 \\ S_n(\lambda_x/4 + L_x/2), & \text{if } \lambda_x/4 + L_x/2 \leq |x| \leq \lambda_x/2 \\ S_n(-x), & \text{if } -(\lambda_x/4 + L_x/2) \leq x \\ & \quad \leq -(\lambda_x/4 - L_x/2). \end{cases} \tag{3}$$

These extensions are identical to those proposed and described in the work of Martinelli and Osella [19].

In the area $0 \leq x \leq \lambda_x/2$, $0 \leq y \leq \lambda_y/2$, $\overline{H}_{\text{ext}}$ coincides with the field produced by the emitter. We extend $\overline{H}_{\text{ext}}$ to the area $-\lambda_x/2 \leq x \leq \lambda_x/2$, $-\lambda_y/2 \leq y \leq \lambda_y/2$ by assuming that its x component is an even function of x and y, and that its y component is an odd function of x and y. Then

$$H_x^{(\text{ext})}(x,y) = \begin{cases} H_x^{(\text{ext})}(-x,y), & \text{if } -\lambda_x/2 \leq x \leq 0,\ 0 \leq y \leq \lambda_y/2 \\ H_x^{(\text{ext})}(x,-y), & \text{if } 0 \leq x \leq \lambda_x/2,\ -\lambda_y/2 \leq y \leq 0 \\ H_x^{(\text{ext})}(-x,-y), & \text{if } -\lambda_x/2 \leq x \leq 0,\ -\lambda_y/2 \leq y \leq 0 \end{cases} \tag{4}$$

$$H_y^{(\text{ext})}(x,y) = \begin{cases} -H_y^{(\text{ext})}(-x,y), & \text{if } -\lambda_x/2 \leq x \leq 0,\ 0 \leq y \leq \lambda_y/2 \\ -H_y^{(\text{ext})}(x,-y), & \text{if } 0 \leq x \leq \lambda_x/2,\ -\lambda_y/2 \leq y \leq 0 \\ H_y^{(\text{ext})}(-x,-y), & \text{if } -\lambda_x/2 \leq x \leq 0,\ -\lambda_y/2 \leq y \leq 0. \end{cases} \tag{5}$$

According to its parity, this field corresponds to the type named as $\overline{H}^{(\mathrm{ext1})}$ in [19].

It is important to point out that the selected extensions neither constrain the type of functions S_n that can be considered inside the studied zone, nor limit the possible orientation of the emitter. Moreover, if λ_x and λ_y are great enough, the imposed parities and periodicities do not affect the response obtained inside the studied area [19].

Assuming that Rayleigh scattering theory is valid on every boundary, the general solutions for the magnetic and electric-field components, which are also periodic with x and y, can be written as the expansions shown at the bottom of the page, where $\gamma_0^2 = -(\omega/c)^2$, $\gamma_n^2 = i\omega\mu_n(\sigma_n + i\omega\varepsilon_n)$, for $1 \le n \le N$, $k_{xl} = 2l\pi/\lambda_x$, $k_{ym} = 2m\pi/\lambda_y$, $[R_{lm}^{(n)}]^2 = k_{xl}^2 + k_{ym}^2 + \gamma_n^2$, $v_{lm}^{++}(x,y) = \cos(k_{xl}x)\cos(k_{ym}y)$, $v_{lm}^{--}(x,y) = \sin(k_{xl}x)\sin(k_{ym}y)$, $v_{lm}^{+-}(x,y) = \cos(k_{xl}x)\sin(k_{ym}y)$, and $v_{lm}^{-+}(x,y) = \sin(k_{xl}x)\cos(k_{ym}y)$. The parities of field components are the same as the ones obtained in [19] for external fields of type 1 and in even interfaces. In that work, only nonmagnetic media were considered, but that result can easily be extended for magnetic media like those considered here. In medium 0, these solutions are valid for (x,y,z) different from (x_e,y_e,z_e). $A_{lm}^{(n)}$ and $B_{lm}^{(n)}$, with $l \ge 0$ and $m \ge 0$, and $C_{lm}^{(n)}$ and $D_{lm}^{(n)}$, with $l > 0$ and $m > 0$, are complex coefficients that depend on frequency ω. $B_{lm}^{(n)}$ and $D_{lm}^{(n)}$ define the incident fields, and $A_{lm}^{(n)}$ and $C_{lm}^{(n)}$ the reflected ones. Therefore

$$H_y^{(\mathrm{ext})}(x,y,0) = l \ge 0, \quad m \ge 0 \sum B_{lm}^{(0)} v_{lm}^{++}(x,y) \tag{12}$$

$$H_y^{(\mathrm{ext})}(x,y,0) = -l > 0, \quad m > 0 \sum D_{lm}^{(0)} v_{lm}^{--}(x,y) \tag{13}$$

$$H_z^{(\mathrm{ext})}(x,y,0) = -l > 0, \quad m \ge 0 \sum \frac{1}{R_{lm}^{(0)}} (k_{xl} B_{lm}^{(0)} + k_{ym} D_{lm}^{(0)}) v_{lm}^{-+}(x,y). \tag{14}$$

These equations determine $B_{lm}^{(0)}$ and $D_{lm}^{(0)}$ because $H_x^{(\mathrm{ext})}$ $x(x,y,0)$and $H_y^{(\mathrm{ext})}(x,y,0)$ are known.

To calculate $A_{lm}^{(0)}$ and $C_{lm}^{(0)}$ as functions of $B_{lm}^{(0)}$, $D_{lm}^{(0)}$, and the earth's structure, we apply the appropriate boundary conditions. On every interface, the tangential components of $\overline{E}$ and $\overline{H}$ are continuous; in the deepest medium, N, $A_{lm}^{(N)}$, and $C_{lm}^{(N)}$ are null for every l and m because the fields must not diverge as z increases. To obtain $A_{lm}^{(0)}$ and $C_{lm}^{(0)}$, we follow a procedure similar to the ones described in the previous works [19], [21].

Due to the range of frequencies used in EMI studies, which are typically in the range 300–20 000 Hz, the process is purely diffusive, and the quasi-stationary approximation is valid. It implies that $\omega\varepsilon_n \ll \sigma_n$ inside the earth. In air, it corresponds to take the limits $\gamma_0 \approx 0$ and $R_{00}^{(0)} \approx 0$, and then [19]

$$A_{00}^{(0)} = B_{00}^{(0)} \tag{15}$$

$$A_{0m}^{(0)} = B_{0m}^{(0)} = 0, \quad \text{if } m > 0 \tag{16}$$

$$k_{ym} A_{lm}^{(0)} = k_{xl} C_{lm}^{(0)}, \quad \text{if } l > 0 \text{ and } m > 0 \tag{17}$$

$$k_{ym} B_{lm}^{(0)} = k_{xl} D_{lm}^{(0)}, \quad \text{if } l > 0 \text{ and } m > 0. \tag{18}$$

Taking into account (18) and (12)–(14), it follows that in the quasi-stationary approximation, $H_y^{(\mathrm{ext})}(x,y,0)$ and $H_z^{(\mathrm{ext})}(x,y,0)$ can be calculated from $H_x^{(\mathrm{ext})}(x,y,0)$. For the source considered here, we have (19), shown at the bottom of the next page. Once $A_{lm}^{(0)}$, $B_{lm}^{(0)}$, $C_{lm}^{(0)}$, and $D_{lm}^{(0)}$ are determined, the induced field in the air $\overline{H}_{\mathrm{ind}}$ can be calculated, and the quotient between the components of $\overline{H}_{\mathrm{ind}}$ and $\overline{H}_{\mathrm{ext}}$, parallel to the magnetic-dipole moment of the receiver $\overline{\mathfrak{M}}_r$ at the receiver location, $\overline{r}_r = (x_r, y_r, z_r)$, can be obtained. Finally, the results are presented as the real and imaginary parts of this quotient, HI and HQ, respectively, expressed in PPM.

$$H_x^{(n)}(x,y,z) = l \ge 0, \quad m \ge 0 \sum \left[A_{lm}^{(n)} \exp\left(R_{lm}^{(n)} z\right) + B_{lm}^{(n)} \exp\left(-R_{lm}^{(n)} z\right) \right] v_{lm}^{++}(x,y) \tag{6}$$

$$H_y^{(n)}(x,y,z) = -l > 0, \quad m > 0 \sum \left[C_{lm}^{(n)} \exp\left(R_{lm}^{(n)} z\right) + D_{lm}^{(n)} \exp\left(-R_{lm}^{(n)} z\right) \right] v_{lm}^{--}(x,y) \tag{7}$$

$$H_z^{(n)}(x,y,z) = l > 0, \quad m \ge 0 \sum \frac{1}{R_{lm}^{(n)}} \left[\left(k_{xl} A_{lm}^{(n)} + k_{ym} C_{lm}^{(n)} \right) \exp\left(R_{lm}^{(n)} z\right) - \left(k_{xl} B_{lm}^{(n)} + k_{ym} D_{lm}^{(n)} \right) \exp\left(-R_{lm}^{(n)} z\right) \right] v_{lm}^{-+}(x,y) \tag{8}$$

$$E_x^{(n)}(x,y,z) = -\frac{i\omega\mu_n}{\gamma_n^2} l > 0, \quad m > 0 \sum \frac{1}{R_{lm}^{(n)}} \left\{ \left[k_{xl} k_{ym} A_{lm}^{(n)} - \left(k_{xl}^2 + \gamma_n^2\right) C_{lm}^{(n)} \right] \exp\left(R_{lm}^{(n)} z\right) - \left[k_{xl} k_{ym} B_{lm}^{(n)} - \left(k_{xl}^2 + \gamma_n^2\right) D_{lm}^{(n)} \right] \exp\left(-R_{lm}^{(n)} z\right) \right\} v_{lm}^{--}(x,y) \tag{9}$$

$$E_y^{(n)}(x,y,z) = \frac{i\omega\mu_n}{\gamma_n^2} l \ge 0, \quad m \ge 0 \sum \frac{1}{R_{lm}^{(n)}} \left\{ \left[(k_{ym}^2 + \gamma_n^2) A_{lm}^{(n)} - k_{xl} k_{ym} C_{lm}^{(n)} \right] \exp\left(R_{lm}^{(n)} z\right) - \left[(k_{ym}^2 + \gamma_n^2) B_{lm}^{(n)} - k_{xl} k_{ym} D_{lm}^{(n)} \right] \exp\left(-R_{lm}^{(n)} z\right) \right\} v_{lm}^{++}(x,y) \tag{10}$$

$$E_z^{(n)}(x,y,z) = -\frac{i\omega\mu_n}{\gamma_n^2} l \ge 0, \quad m > 0 \sum \left[\left(-k_{ym} A_{lm}^{(n)} + k_{xl} C_{lm}^{(n)} \right) \exp\left(R_{lm}^{(n)} z\right) + \left(-k_{ym} B_{lm}^{(n)} + k_{xl} D_{lm}^{(n)} \right) \exp\left(-R_{lm}^{(n)} z\right) \right] v_{lm}^{+-}(x,y) \tag{11}$$

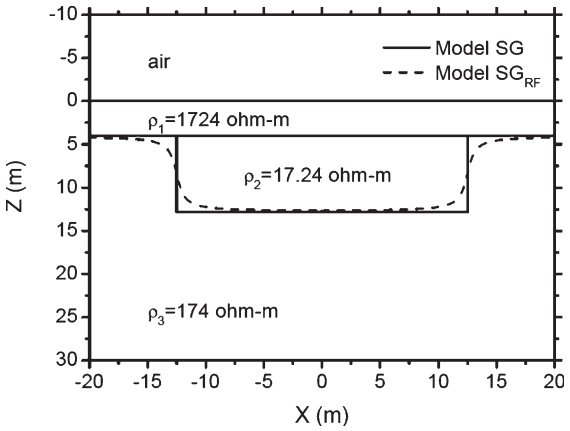

Fig. 1. Model proposed by Stoyer and Greenfield [6] (Model SG) together with the smoothed version of that model employed here to apply the RF method (Model $\mathrm{SG_{RF}}$).

It is worth to mention that, for the sake of simplicity, the user of the code can select an arbitrary location of the studied area. The user enters that location and the values of λ_x and λ_y, and the code automatically shifts the center of the area to the point $(x, y) = (\lambda_x/4, \lambda_y/4)$ and generates the extended model that satisfies all the assumptions described before.

III. Validation of the Method

Rayleigh scattering theory is an approximation valid when the boundary slopes are not too large because multiple reflections are not contemplated. Considering this, we extensively tested our 2-D and 3-D RF magnetotelluric modeling methods [20], [21], by comparison with other existing FD, FE, and IE solutions, in order to find a self-consistency criterion for the determination of the validity of Rayleigh's solutions in each particular case. We found that when Rayleigh's approximation is valid, the series expansion of field components is convergent and then the coefficients corresponding to l or m greater than a finite value L can be neglected. In these cases, the root mean-squared values of the residual discontinuities of the tangential components at layer boundaries can be reduced to a level below a few points per cent by increasing the number of scattering orders L. On the contrary, when the approximation is no more valid, the series exhibit oscillatory or even divergent behavior, and the residual discontinuities always remain large. The maximum boundary slopes that can be correctly modeled using RF techniques, in the magnetotelluric case, which corresponds to uniform external fields, lie typically in the range $50°-60°$ but can exceed these values for very resistive media. For the RF method proposed here as for the one presented in [19], we obtained convergent solutions and low residual discontinuities for a similar range of boundary slopes.

For 1-D structures, we verified that, like the magnetotelluric case, convergent solutions and low residual discontinuities effectively correspond to valid Rayleigh solutions. This was done by comparing the responses calculated with our method to the ones obtained with the EM1DFM code developed at the University of British Columbia (UBC) [22], and based on the work of Farquharson *et al.* [5], for a great number of 1-D models.

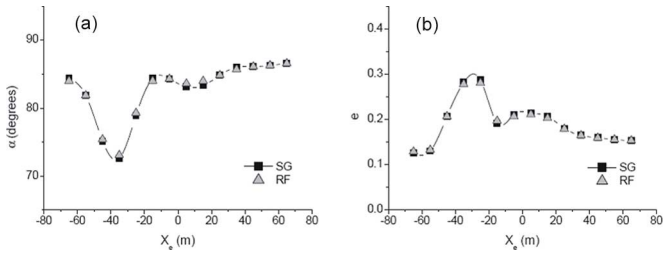

Fig. 2. Comparison between the response of Model SG published by Stoyer and Greenfield [6] (SG) and the response of Model $\mathrm{SG_{RF}}$ calculated using the RF method (RF). The axes of the emitter and receiver dipoles are parallel to the x direction.

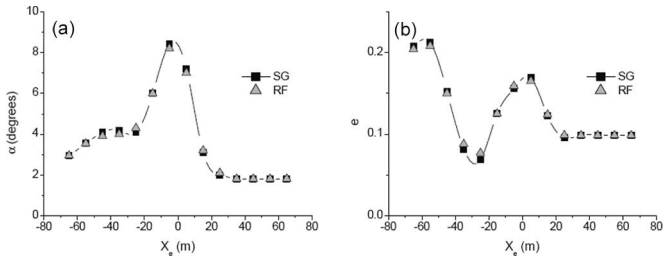

Fig. 3. Comparison between the response of Model SG published by Stoyer and Greenfield [6] (SG) and the response of Model $\mathrm{SG_{RF}}$ calculated using the RF method (RF). The axes of the emitter and receiver dipoles are parallel to the z direction.

At least to our knowledge, there are no recently published modeling methods for 2-D structures and magnetic-dipole sources. Therefore, for 2-D structures, we compared our solutions to some of the results published by Stoyer and Greenfield [6]. We selected the model shown in [6, Fig. 20]. Fig. 1 displays that model (Model SG), together with a smoothed version of it (Model $\mathrm{SG_{RF}}$), which we employed to apply our RF code. We smoothed the boundaries of the original model because, as we explained previously in this section, our method does not include vertical contacts. Figs. 2 and 3 compare the response of Model $\mathrm{SG_{RF}}$, calculated using the RF method, to the response of Model SG, published by those authors. The emitter and the receiver are located at positions $\overline{r}_e = (x_e, 0, -2m)$ and $\overline{r}_r = (x_e + 35m, 0, -2m)$, respectively. The frequency is 27.7 kHz. $\overline{\overline{\mathfrak{M}}}_e$ and $\overline{\overline{\mathfrak{M}}}_r$ are oriented in the x direction in Fig. 2, and in the z direction in Fig. 3. Instead of HI and HQ, the tilt angle α and the ellipticity e, of the polarization ellipse of the magnetic field detected by the receiver, are plotted as functions of x_e (x_e is 0 when the emitter is just over the center of the structure). The agreement between both solutions is remarkable, in spite of the smoothing of the original model.

$$H_x^{(\mathrm{ext})}(x, y, 0) = \frac{1}{4\pi} \frac{\mathfrak{M}_x^{(e)} \left[2(x - x_e)^2 - (y - y_e)^2 - z_e^2\right] + \mathfrak{M}_y^{(e)} 3(x - x_e)(y - y_e) + \mathfrak{M}_z^{(e)} 3(x - x_e)(-z_e)}{\left[(x - x_e)^2 + (y - y_e)^2 + z_e^2\right]^{5/2}} \tag{19}$$

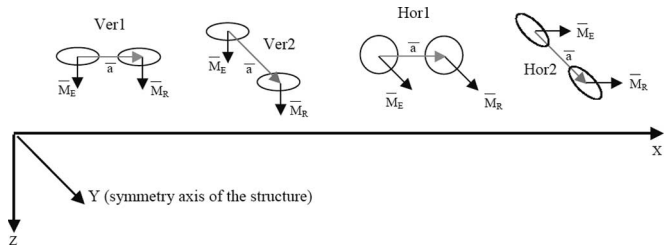

Fig. 4. Instrument's configurations Ver1, Ver2, Hor1, and Hor2.

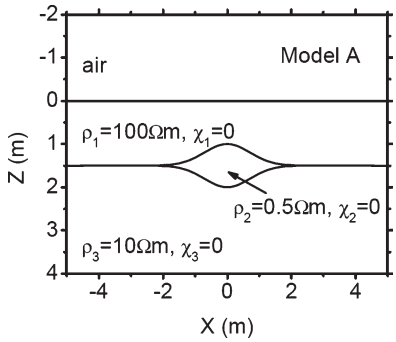

Fig. 5. Model A representing a 2-D conductive body embedded in a more resistive two layer host.

IV. Modeling a Buried Nonmetallic 2-D Body

In this section, we use our code to calculate the synthetic responses of a buried nonmetallic 2-D body for different dipole orientations. The body is conductive with respect to the host media. We analyze the sensitivity of the responses in order to determine which configuration best characterizes this body.

We assume that we have a system such that $\overline{\overline{\mathfrak{M}}}_e$ and $\overline{\overline{\mathfrak{M}}}_r$ are parallel, and both are perpendicular to the direction of the instrument's axis $\overline{a} = \overline{r}_r - \overline{r}_e$. The distance between the dipoles is $|\overline{a}| = 1.67$ m. The center of this system is $\overline{c} = (x_c, y_c, z_c) = (\overline{r}_r + \overline{r}_e)/2$. $\overline{c}$ is moved along the x axis, which is perpendicular to the symmetry axis of the structure, such that $y_c = 0$ and $z_c = -1$ m. We consider four instrument configurations, named Ver1, Ver2, Hor1, and Hor2, which are shown in Fig. 4.

Fig. 5 shows the soil model named model A. The embedded body is more conductive than the host media, and the magnetic susceptibilities are all equal to zero. The interfaces $z = S_n(x)$, for $n = 1$ and 2, are given by

$$z = S_n(x) = P + \Delta Z_n \exp\left[-(x/G)^2\right] \qquad (20)$$

with $P = 1.5$ m, $G = 1$ m, $\Delta Z_1 = -0.5$ m, and $\Delta Z_2 = 0.5$ m.

Fig. 6 shows the HI and HQ components of the EMI responses of model A, plotted as functions of x_c, for the four configurations (x_c is zero just over the center of the body). Also, the responses obtained after removing the body for the vertical and horizontal configurations, 1D-Ver and 1D-Hor, respectively, are shown. The responses are all symmetrical with respect to $x_c = 0$; hence, the results are given only for $x_c \geq 0$. For all the configurations, the responses exhibit positive anomalies with respect to the results that are obtained without the body. Over the body, the greatest anomalies correspond to the configuration Hor2. This configuration has the best sensitivity to the presence of the body and gives the best delimitation of its lateral width. The sensitivity of the configuration Hor1 is much lower than that of the configuration Hor2. For the configurations Ver1 and Ver2, the HI and HQ components have a local minimum over the center of the body and have a maximum near each lateral border located at $|x_c| \approx 2$ m. The anomalies extend up to values of $|x_c|$ as great as, approximately, 10 m.

V. Modeling of a Contaminant Plume

We also used our method to analyze data from a contaminated site, due to a hydrocarbon spill. In that zone, electrical and EMI data were collected along several profiles. The electrical profiles were acquired using the multielectrode resistivimeter Saris 500. Dipole–dipole arrays were deployed with apertures of 3 m. EMI data were acquired along the same profiles using a multifrequency EM profiler GEM-300 [23]. These data were collected with a step of 3 m, for a frequency range 330–19 975 Hz, in the configuration Ver1.

From the inversion of geoelectrical data, electrical images were obtained. The inversions were made applying the DCIP2D inversion code of the UBC [24], and based on the work of Oldenburg *et al.* [25] and Oldenburg and Li [26].

We interpreted EMI data from one of these profiles, where a resistive anomaly that could be associated to the presence of the contaminant plume was clearly mapped from the electrical inversion (Fig. 7). First, we built a starting multilayer representation of the soil structure shown in Fig. 7 and calculated its synthetic EMI response using our code; then, we varied this model, using a trial-and-error procedure, until a good correlation between the data and the synthetic response was achieved for all the measured frequencies. Fig. 8 shows the final model, and Fig. 9 compares its synthetic response to the data at 19 975 Hz. The computation time for obtaining the synthetic response of this model, at this frequency and for all the source locations, was approximately 15 min on a personal computer with an Intel Pentium IV (2.4 GHz) processor.

VI. Conclusion

We developed a 2.5-D forward method to calculate the dual-coil frequency-domain EMI response of 2-D multilayered structures with irregular interfaces based on RF expansions. This method is user friendly. When boundary slopes are lower than $50^\circ - 60^\circ$, it has good convergence and computation costs easily affordable for present-day personal computers. In these cases, it gives reliable results.

Applying this method, we calculated the synthetic response of a buried nonmetallic body, conductive with respect to the host media, for four possible measurement configurations. The greatest anomaly is obtained when the magnetic-dipole moments are horizontal and perpendicular to the strike direction of the structure, and the axis of the instrument is parallel to the strike (configuration Hor2). The lateral extension of this anomaly is similar to the width of the body. Then, for a qualitative interpretation made just from visualization of the data, configuration Hor2 will best detect the body and delimit its width. As the rest of the configurations give less localized anomalies, the width of the body would be overestimated.

Finally, we used our code and a trial-and-error procedure to model field data acquired along a profile crossing a

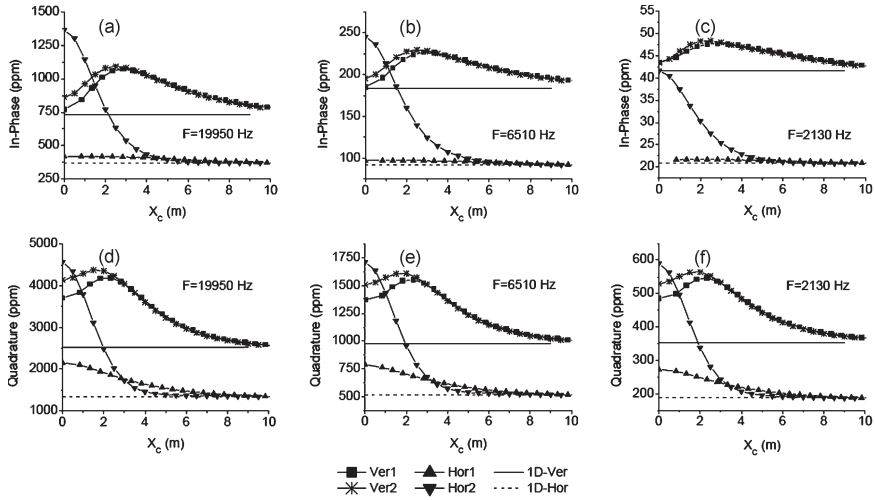

Fig. 6. Responses of model A calculated for the configurations Ver1, Ver2, Hor1, and Hor2 together with the responses obtained after removing the body for configurations Ver1 and Ver2 (1D-Ver) and Hor1 and Hor2 (1D-Hor).

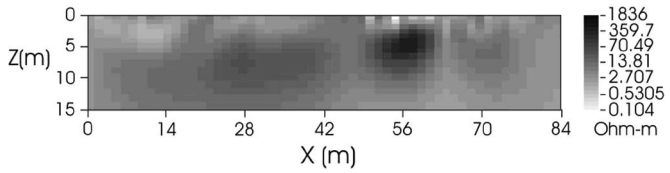

Fig. 7. Structure of the subsoil below the studied profile obtained through 2-D inversion of geoelectrical data.

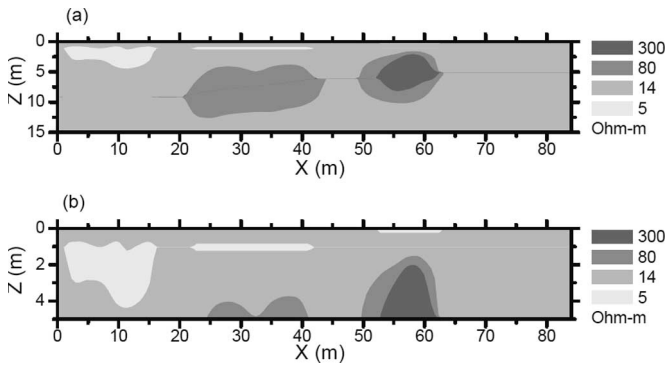

Fig. 8. (a) Multilayer representation of the structure shown in Fig. 7. (b) Upper 5-m depth of this model.

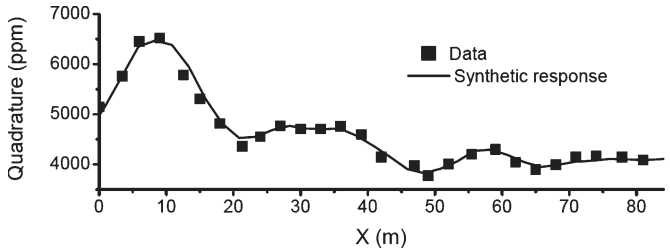

Fig. 9. Synthetic response of the model shown in Fig. 8 for configuration Ver1, at 19 975 Hz, compared to the corresponding data.

contaminated zone. In this zone, a hydrocarbon spill produced a localized plume of enhanced resistivity. The first characterization of this profile had been obtained from the inversion of dipole–dipole electrical data. We considered that result to build our starting layered model. We obtained a good correlation between the EMI data and the synthetic response of the final model, which also is consistent with the image of the electrical inversion. During the modeling process, the method showed to be practical and versatile, and had a good convergence.

REFERENCES

[1] N. Geng, C. E. Baum, and L. Carin, "On the low-frequency natural response of conducting and permeable targets," *IEEE Trans. Geosci. Remote Sens.*, vol. 37, no. 1, pp. 347–359, Jan. 1999.

[2] C. O. Ao, H. Braunisch, K. O'Neill, and J. A. Kong, "Quasi-magnetostatic solution for a conducting and permeable spheroid with arbitrary excitation," *IEEE Trans. Geosci. Remote Sens.*, vol. 40, no. 4, pp. 887–897, Apr. 2002.

[3] F. Shubitidze, K. O'Neill, S. A. Haider, K. Sun, and K. D. Paulsen, "Application of the method of auxiliary sources to the wide-band electromagnetic induction problem," *IEEE Trans. Geosci. Remote Sens.*, vol. 40, no. 4, pp. 928–942, Apr. 2002.

[4] K. Sun, K. O'Neill, F. Shubitidze, I. Shamatava, and K. D. Paulsen, "Theoretical analysis and range of validity of TSA formulation for application to UXO discrimination," *IEEE Trans. Geosci. Remote Sens.*, vol. 42, no. 9, pp. 1871–1881, Sep. 2004.

[5] C. G. Farquharson, D. W. Oldenburgh, and P. S. Routh, "Simultaneous 1D inversion of loop–loop electromagnetic data for magnetic susceptibility and electrical conductivity," *Geophysics*, vol. 68, no. 6, pp. 1857–1869, Nov./Dec. 2003.

[6] C. H. Stoyer and R. J. Greenfield, "Numerical solutions of the response of a two-dimensional earth to an oscillating magnetic dipole source," *Geophysics*, vol. 41, no. 3, pp. 519–530, 1976.

[7] K. H. Lee and H. F. Morrison, "A numerical solution for the electromagnetic scattering by a two-dimensional inhomogeneity," *Geophysics*, vol. 50, no. 3, pp. 466–472, Mar. 1985.

[8] J. Doherty, "EM modelling using surface integral equations," *Geophys. Prospect.*, vol. 36, no. 6, pp. 644–668, 1988.

[9] K. H. Lee, D. F. Pridmore, and H. F. Morrison, "A hybrid three-dimensional electromagnetic modeling scheme," *Geophysics*, vol. 46, no. 5, pp. 796–805, May 1981.

[10] D. F. Pridmore, G. W. Hohmann, S. H. Ward, and W. R. Sill, "An investigation of finite-element modeling for electrical and electromagnetic data in three dimensions," *Geophysics*, vol. 46, no. 7, pp. 1009–1024, Jul. 1981.

[11] G. W. Hohmann, "Three-dimensional EM modeling," *Geophys. Surv.*, vol. 6, no. 1/2, pp. 27–53, Jul. 1983.

[12] G. A. Newman and D. L. Alumbaugh, "Frequency-domain modeling of airborne electromagnetic responses using staggered finite differences," *Geophys. Prospect.*, vol. 43, no. 8, pp. 1021–1042, 1995.

[13] ——, "Three-dimensional massively parallel electromagnetic inversion—I: Theory," *Geophys. J. Int.*, vol. 128, no. 2, pp. 345–354, 1997.

[14] Y. Sasaki, "Full 3-D inversion of electromagnetic data on PC," *J. Appl. Geophys.*, vol. 46, no. 1, pp. 45–54, Jan. 2001.

[15] M. J. Unsworth, B. J. Travis, and A. D. Chave, "Electromagnetic induction by a finite electric dipole source over a 2-D earth," *Geophysics*, vol. 58, no. 2, pp. 198–214, Jan. 1993.
[16] Y. Mitsuhata, "2-D electromagnetic modeling by finite-element method with a dipole source and topography," *Geophysics*, vol. 65, no. 2, pp. 465–475, Mar./Apr. 2000.
[17] Y. Mitsuhata, T. Uchida, and H. Amano, "2.5-D inversion of frequency-domain electromagnetic data generated by a grounded-wire source," *Geophysics*, vol. 67, no. 6, pp. 1753–1768, Nov./Dec. 2002.
[18] C. De Groot-Hedlin and S. Constable, "Inversion of magnetotelluric data for 2D structure with sharp resistivity contrasts," *Geophysics*, vol. 69, no. 1, pp. 78–86, Jan./Feb. 2004.
[19] P. Martinelli and A. Osella, "Modelling electromagnetic responses of 2-D structures due to spatially non-uniform inducing fields. Analysis of magnetotelluric source effects at coast lines," *Geophys. J. Int.*, vol. 155, no. 2, pp. 623–640, Nov. 2003.
[20] A. Osella and P. Martinelli, "Magnetotelluric responses of anisotropic bidimensional structures," *Geophys. J. Int.*, vol. 115, no. 3, pp. 819–828, 1993.
[21] P. Martinelli and A. M. Osella, "MT forward modeling of 3D anisotropic electrical conductivity structures using the Rayleigh–Fourier method," *J. Geomagn. Geoelectr.*, vol. 49, no. 11, pp. 1499–1518, 1997.
[22] *EM1DFM V1.0, Inversion and Modeling of Applied Geophysical Electromagnetic Data*, 2000, Vancouver, BC, Canada: UBC-Geophysical Inversion Facility.
[23] I. J. Won, D. A. Kreiswetter, G. R. A. Fields, and L. Sutton, "GEM-2: A new multifrequency electromagnetic sensor," *J. Environ. Eng. Geophys.*, vol. 1, no. 2, pp. 129–137, 1996.
[24] *DCIP2D V3.1, Forward Modelling and Inversion of DC Resistivity and Induced Polarization Data Over 2D Structures*, 2001, Vancouver, BC, Canada: UBC-Geophysical Inversion Facility.
[25] D. W. Oldenburg, P. R. McGillivary, and R. G. Ellis, "Generalized subspace method for large scale inverse problems," *Geophys. J. Int.*, vol. 114, no. 1, pp. 12–20, 1993.
[26] D. W. Oldenburg and Y. Li, "Inversion of induced polarization data," *Geophysics*, vol. 59, no. 9, pp. 1327–1341, Sep. 1994.

Patricia Martinelli received the Ph.D. degree in physics from the University of Buenos Aires, Buenos Aires, Argentina, in 1994.

She is currently an Associate Research Scientist in the National Research Council Consejo Nacional de Investigaciones Científicas y Técnicas (CONICET), Buenos Aires, and a member of the Physics Department of the Faculty of Sciences, University of Buenos Aires. Her main research interests include the development of 2-D and 3-D electromagnetic modeling codes and the study of the electrical properties of the crust and upper mantle in the South American subduction zone.

Ana Osella received the Ph.D. degree in physics from the University of Buenos Aires, Buenos Aires, Argentina, in 1983.

Since 1984, she has been a Research Scientist in the National Research Council and Professor in the Faculty of Sciences of the University of Buenos Aires. Since 1988, she has been the Head of the Applied and Environmental Geophysics group. Her research activities are in the fields of EM induction in the earth: EM and DC measurements for upper crustal studies and also to environmental and engineering applications, continental lower crustal studies through EM data, and seismicity.

Eugenia Lascano received the "licenciatura" (equivalent to Master in Science) degree in physics from the University of Buenos Aires, Buenos Aires, Argentina, in 2001. She is currently working toward the Ph.D. degree at the University of Buenos Aires.

She is a Teaching Assistant at the University of Buenos Aires. She is working at the Applied and Environmental Geophysics Group from that university. Her research interests are the application of EM geophysical methods to archaeology and underground contamination problems, data processing and imaging, and EM modeling.